On the Range of Water Structure Models Compatible with X-ray and Neutron Diffraction Data

ARTICLE *in* THE JOURNAL OF PHYSICAL CHEMISTRY B · MAY 2009

Impact Factor: 3.3 · DOI: 10.1021/jp9007619 · Source: PubMed

5 AUTHORS, INCLUDING:

Kjartan Thor Wikfeldt
University of Iceland
29 PUBLICATIONS **730** CITATIONS
SEE PROFILE

Mathias P Ljungberg
Donostia International Physics Center
28 PUBLICATIONS **934** CITATIONS
SEE PROFILE

Lars G M Pettersson
Stockholm University
318 PUBLICATIONS **11,042** CITATIONS
SEE PROFILE

THE JOURNAL OF PHYSICAL CHEMISTRY B

Article

On the Range of Water Structure Models Compatible with X-ray and Neutron Diffraction Data

Kjartan T. Wikfeldt, Mikael Leetmaa, Mathias P. Ljungberg, Anders Nilsson, and Lars G. M. Pettersson

J. Phys. Chem. B, **2009**, 113 (18), 6246-6255• DOI: 10.1021/jp9007619 • Publication Date (Web): 09 April 2009

On the Range of Water Structure Models Compatible with X-ray and Neutron Diffraction Data

Kjartan T. Wikfeldt,[†] Mikael Leetmaa,[†] Mathias P. Ljungberg,[†] Anders Nilsson,[†,‡] and Lars G. M. Pettersson*,[†]

FYSIKUM, AlbaNova University Center, Stockholm University, SE-106 91 Stockholm, Sweden, and Stanford Synchrotron Radiation Laboratory, P.O. Box 20450, Stanford, California 94309

Received: January 26, 2009

We use the reverse Monte Carlo (RMC) method to critically evaluate the structural information content of diffraction data on bulk water by fitting simultaneously or separately to X-ray and neutron data; the O−H and H−H, but not the O−O, pair-correlation functions (PCFs) are well-described by the neutron data alone. Enforcing at the same time different H-bonding constraints, we generate four topologically different structure models of liquid water, including a simple mixture model, that all equally well reproduce the diffraction data. Although earlier work [Leetmaa, M.; et al. *J. Chem. Phys.* **2008**, *129*, 084502] has focused on tetrahedrality in the H-bond network in liquid water, we show here that, even for the O−O−O three-body correlation, tetrahedrality is not strictly defined by the data. We analyze how well two popular MD models (TIP4P-pol2 and SPC/E) reproduce the neutron data in *q*-space and find differences in important aspects from the experiment. From the RMC fits, we obtain pair-correlation functions (PCFs) that are in optimal agreement with the diffraction data but still show a surprisingly strong variability both in position and height of the first intermolecular (H-bonding) O−H peak. We conclude that, although diffraction data impose important constraints on the range of possible water structures, additional data are needed to narrow the range of possible structure models.

Introduction

There is currently a debate regarding the structure of water at ambient conditions (see the discussion in ref 1). This was initiated by the Wernet et al. study[2] using X-ray absorption spectroscopy (XAS) and X-ray Raman scattering (XRS) that inferred a structure with a much weaker hydrogen bond (H-bond) connectivity than what is seen in most molecular dynamics (MD) simulations. It is therefore extremely important that we can evaluate what strict bounds other experimental data really provide regarding the structure. The most direct experimental information about the liquid structure is usually obtained from various diffraction methods.[3−5] Due to the limited *q*-range in the X-ray diffraction experiments and the fact that the intramolecular scattering makes a dominating contribution already at relatively low momentum transfer in neutron diffraction, there is, however, no straightforward way to convert the experimental data into a unique structural solution. Various structure models can, on the other hand, be evaluated through a comparison with experiment in *q*-space. If a satisfactory agreement has been reached in this comparison, the O−O, O−H, and H−H pair-correlation functions (PCF) can be extracted. What is not known at this point, however, is the range of possible structure models that are not contradicted by the data and how large variations are in the corresponding PCFs that are compatible with the existing diffraction data.

In a recent study,[6] we used the reverse Monte Carlo (RMC) modeling technique to explore what bounds, in terms of H-bonding that X-ray[7] and neutron diffraction data,[5] together with the E-field distribution from a TIP4P-pol2 simulation[8] as a representation of the Raman spectrum in the OH-stretch region of dilute HOD in D_2O,[9] actually set on water structure models. Two extreme structure models for liquid water were generated by maximizing either the number of tetrahedrally or asymmetrically H-bonded molecules while still fitting the data. In addition, the internal structures were constrained to reproduce the quantum distributions of distances and angles.[10] The data were found to allow a surprisingly large range of structure models in terms of H-bond statistics; even the combination of X-ray, neutron, and Raman data was found to only constrain the H-bond statistics in structure models to the range from 80% double donor (DD) and 20% single donor (SD) to 20% DD and 80% SD according to the H-bond definition in Wernet et al.;[2] in terms of the number of H-bonds, the range was 3.41−2.35 with the same H-bond definition[2] applied to both models. The first peak in the O−O pair correlation was found, in agreement with an earlier study using the empirical potential structure refinement (EPSR) approach,[5] to be significantly lower and broader than typically obtained from molecular dynamics (MD) simulations, indicating that MD potentials need to be softer to reproduce the experimental diffraction data.[5]

Since the previous study we have gained two essential insights that indicate that we have not fully explored the range of structure models that the diffraction data would allow. We have, in a theoretical study of the OH stretch frequency distributions[11] in water, seen that there are serious questions regarding the validity of the *E*-field distribution as a quantitative model for the OH stretch of dilute HDO in D_2O. Although there is an overall, albeit model-dependent, correlation between *E*-field and frequency, any given value of the *E*-field can be mapped onto a frequency range broader than the entire spectrum.[11]

Furthermore, as shown in the present study, using the *E*-field distribution from an MD simulation as a constraint in our

* To whom correspondence should be addressed. E-mail: lgm@physto.se.
† Stockholm University.
‡ Stanford Synchrotron Radiation Laboratory.

10.1021/jp9007619 CCC: $40.75
Published on Web 04/09/2009

previous study[6] resulted in structures that were very different in terms of H-bond tetrahedrality yet very tetrahedral in terms of the O−O−O angles reflecting the TIP4P-pol2 simulation from which the *E*-field distribution was obtained. This tetrahedrality, however, is not actually given by the experimental data but is a result of the assumed *E*-field distribution; since the connection between *E*-field distribution and distribution of actual frequencies depends on the structure model,[11] an assumed shape of the *E*-field distribution biases the fit toward the particular theoretical model from which it was derived. Considering these uncertainties it is therefore extremely important to investigate if other structure models that are much less tetrahedral also in terms of the O−O−O angle are also consistent with the experimental diffraction data. Second, recent X-ray emission spectroscopy (XES) data on water[1] indicate a bimodal distribution around two rather distinct different local H-bond configurations, either tetrahedral or very distorted; this is also supported by the previous X-ray absorption spectroscopy (XAS) study.[2] These could be homogeneously distributed or indicative of heterogeneities in the liquid, and it thus becomes important to investigate if either possibility is contradicted by diffraction data. As a first approximation, it was assumed in the XES study[1] that if two different structure models can describe the diffraction data, a linear combination of them should also provide a good fit. However, it is essential to confirm this assumption through explicitly fitting a mixture of structures that have rather different H-bond connectivity, as will be done in the present work.

Here we thus extend our previous structural analysis of MD and RMC structure models and look in detail at the O−O, O−H, and H−H correlations in both *r*- and *q*-space to gain an understanding of what structure information can strictly be derived from diffraction data. The tetrahedrality of the studied structure models in terms of oxygen positions, as opposed to H-bonds, is also investigated through the distribution of O−O−O angles.

Diffraction experiments on water have a long history, but the interpretation of the resulting diffraction pattern has remained a challenging task. One of the first attempts to explain the peculiar properties of water from its microscopic structure was made by Röntgen, who in 1892 proposed that the liquid consisted of one icelike component and one unknown.[12] In 1938, however, Morgan and Warren[13] stated that their X-ray diffraction (XD) data supported the view of water being tetrahedrally structured. Their view was strongly influenced by the pioneering work of Bernal and Fowler in 1933,[14] who interpreted early measurements of the X-ray diffraction pattern of water (see ref 14 and references therein) as sure indications that water is indeed tetrahedral and icelike. Since the current debate about water structure[1,2,15−34] is quite reminiscent of the situation around half a century ago, it can be illuminating to reconsider the conclusions drawn back then on the basis of XD data.

In 1969, Narten and Levy took a step further in the evaluation of XD data when they, in a systematic way, discriminated between proposed structure models.[35] Their conclusion[35] was that, given the available suggestions for the structure of water at that time, only the tetrahedral icelike model was detailed enough to be tested and was also found consistent with experimental data. This and the earlier influential papers[13,14] played a crucial role in establishing the tetrahedral model as the currently accepted description of water structure.

The method of data analysis at that time consisted of Fourier transforming the XD structure factor to obtain the PCF in *r*-space and utilizing the thus acquired distances and coordination numbers to discriminate between structure models. Nowadays, it is easy to create large structure models (in the sense of a large periodic box of molecules) and transform to *q*-space to check their consistency with diffraction data. One can thus, in a much more rigorous and systematic way than before, establish which structure models for liquid water actually do agree with diffraction data and explore what bounds the experimental data impose on structure models. The RMC method[36] has been used for this purpose before, where it was shown that RMC in general produces a maximally disordered structure where higher-order correlations are not necessarily reproduced,[37] that MD models need to be improved to reproduce diffraction experiments,[38] and that reported experimental partial PCFs (PPCF) are poorly determined by the then available ND data sets.[39] Also the Empirical Potential Structure Refinement (EPSR) method[40] has been applied, demonstrating that diffraction data are unable to discriminate between effective pair-potential models with either symmetrical or asymmetrical charges within the water molecules[32] and that pair-potentials need to be softer and the first O−O peak in the PPCF, $g_{OO}(r)$, lower than reported from MD simulations.[5] Since unbiased structural information from diffraction experiments is extremely important, we found the need for a thorough analysis of the structural content of the XD and ND data on water to be quite pressing.

Here we report on structure modeling using RMC of the XD pattern of water, as measured by Hura et al.,[7] and five ND data sets on different isotopic mixtures of water by Soper.[5] In the context of these most recent diffraction data sets, we also report on a detailed structural analysis of two popular MD models of water, namely, TIP4P-pol2[8] and SPC/E,[41] where in particular the TIP4P-pol2 model has been suggested to give a distribution of structures that is representative of the real liquid.[7] In this context, it is advisible that the comparison to experiment is performed in *q*-space since all experimentally derived $g(r)$ functions are inherently subject to large uncertainties due to the Fourier transform over a limited *q*-interval; taking the atomistic real-space structure of the MD model to *q*-space is, on the other hand, straightforward.

RMC modeling[36] is a well-known general method of fitting structure models to experimental structural data. Traditionally, RMC has been used to extract structural information such as PCFs, coordination numbers, and bond-angle distributions, from diffraction experiments.[36] Although mainly X-ray and neutron diffraction data have been used,[42] the general nature of the RMC algorithm allows any data to be modeled, given that it can be calculated from an atomistic structure. More indirect structural information from experiments can be included through the use of geometrical constraints. No intermolecular potential based on a priori assumptions about the interactions is applied, contrary to the case of the complementary EPSR method, where as much physics as possible is intentionally built into the analysis through the starting potential.[5] RMC, on the other hand, makes as few a priori assumptions as possible[43] and furthermore allows introducing geometrical constraints, which can be conveniently used to examine the range of structure models that can be accommodated by the data, and the uncertainties in the PPCFs can be evaluated. This is more difficult in the EPSR approach, in which only the starting potential is available to drive the fit toward a particular solution to explore bounds on structure models. In one such study,[32] however different initial potentials were applied in EPSR fits to diffraction data on water, and indeed, different structural solutions and final potentials were found.

The RMC procedure strives to generate structures that reproduce the experimental data, but the resulting structures are

not necessarily correct or even thermodynamically accessible.[44,45] However, contrary to EPSR, it is only constrained by the data and specifically introduced geometrical constraints, thus providing a convenient means to explore what bounds in terms of possible structure distributions the experiments impose. Using RMC we have thus here created four structure models, widely different in terms of H-bond connectivity, showing differences in the O−O−O angles and even differing in important details of the PPCFs, that all, however, show an equal goodness of fit to experimental X-ray and neutron diffraction data in q-space.

Methods

A. RMC Fitting. One of the main ideas behind the development of the RMC algorithm was to replace the direct $q \rightarrow r$ Fourier transform of diffraction data with the inverse $r \rightarrow q$ transform, thus avoiding truncation errors caused by the finite q-interval of the experiment and reducing the effect of possible systematic errors in the data[36] by basing the analysis on an atomistic structure model. We emphasize, however, that while a very large simulation box in r-space eliminates mathematical problems associated with taking the Fourier transform, it does not improve the r-space resolution, which is determined by the experimental data in q-space; this is still set by the approximate relation $\Delta r \sim 2\pi/q_{\max}$, where $q_{\max}$ is the highest q-value measured.

The X-ray and neutron diffraction patterns are calculated via the partial structure factors (PSFs), $A_{\alpha\beta}(q)$, obtained by Fourier transforming the radial distribution functions:

$$A_{\alpha\beta}(q) = 1 + 4\pi\rho \int r^2 [g_{\alpha\beta}(r) - 1] \frac{\sin(qr)}{qr}\, \mathrm{d}r \qquad (1)$$

where $g_{\alpha\beta}(r)$ is the partial PCF for atoms of types α and β, and ρ is the atomic number density. The total structure factors are then formed as weighted combinations of the PSFs, with the weights given in the case of neutrons by the atomic scattering lengths and for X-rays by the q-dependent form factors,

$$S_{\mathrm{ND}}(q) = \sum_{\alpha} \sum_{\beta} (2 - \delta_{\alpha\beta}) c_\alpha c_\beta \langle b_\alpha \rangle \langle b_\beta \rangle (A_{\alpha\beta}(q) - 1) \quad (2)$$

$$S_{\mathrm{XD}}(q) = \sum_{\alpha} \sum_{\beta} (2 - \delta_{\alpha\beta}) c_\alpha c_\beta f_\alpha(q) f_\beta(q) - (A_{\alpha\beta}(q) - 1) / \sum_i c_i f_i^2(q) \quad (3)$$

where c_i is the concentration of atomic species i in the sample, the Kronecker δ function avoids double counting, $f_i(q)$ are the atomic form factors, $\langle b_i \rangle$ are the atomic scattering lengths, and the angular brackets denote the spin and isotopic average.

Note that RMC includes the intramolecular distances in the PSFs, so the intramolecular scattering is included in the total structure factors above. It is straightforward in the case of neutron diffraction to calculate the weights of the different partial correlations through the atomic scattering lengths. These scattering lengths are constants that only depend on the type of nucleus. Hydrogen and its isotope deuterium have widely different scattering lengths, a fact that facilitates the use of neutron diffraction to, by isotopic substitution, separate out the PSFs in methods such as RMC and EPSR. A problem that is encountered, however, is the large inelastic scattering background for hydrogen, which makes the oxygen−oxygen correlation hard to determine solely from neutron diffraction data.[39] This is where the XD data provide the most important complementary information. Another potential source of error, when using isotopic mixtures, is the structural difference between H_2O and D_2O,[46−49] which might average out certain aspects of the structure.

TABLE 1: Contribution of Each PSF to the Total ND Structure Factors[a]

data set	% O−O	% O−H	% H−H
100% D_2O	9.2	42.3	48.6
75% D_2O	17.3	48.6	34.1
50% D_2O	44.1	44.6	11.3
25% D_2O	51.6	40.4	8.0
100% H_2O	19.1	49.2	31.7

[a] Note that the O−H partial added in is negative for the two most hydrogenous samples.

The influence of each partial correlation in the neutron structure factors expressed as a percentage for each data set is shown in Table 1 and will be used below to decompose the structural information in the data. Note that for the two most hydrogenous samples the O−H PSF is added with a negative weight, hence the totally different scattering profiles of D_2O and H_2O.

The calculation of the X-ray total structure factor relies, in this formalism, on the spherical atom approximation, in which the independent atomic form factors, IAFFs, are the Fourier transform of the atomic electron density. Since the formation of chemical bonds modifies the electronic structure of the atoms, with an accumulation of charge on the oxygen atom in the case of water, the IAFF approximation can become quite poor. This problem has been addressed by Head-Gordon and co-workers in ref 50, where a modification of the IAFFs was suggested, in which the form factors are modified at low q to account for charge transfer and valence electron delocalization. We apply here the same parameters as in refs 50 and 6, which were previously found to give the best fit within this modification scheme.

For all RMC fitting, a locally modified version of the RMC++ code[51] has been used. The joint XD and ND RMC fits were performed with the room temperature XD data set of Hura et al.[7] and five neutron diffraction data sets from Soper,[5] measured on the isotopic mixtures 100% D_2O, 75% D_2O 25% H_2O, 50% D_2O 50% H_2O, 25% D_2O 75% H_2O, and 100% H_2O. The data treatment and normalization were the same as in ref 6. In order to investigate the structural information content in just the neutron diffraction data, RMC fits were also performed without the XD data.

All simulations investigating differently H-bonded models were performed with a box-length of 82.082 Å and 18 432 water molecules (giving a number density of 0.1 atoms/Å^3, i.e. a room temperature density of 0.997 g/cm^3), using distances up to 20 Å in the Fourier transform of $g(r)$. The size of the simulation boxes ensured good statistics in the PPCFs.

B. H-Bonds and Intramolecular Geometries. To be able to investigate the sensitivity of the data to the H-bonding configurations in water, modifications of the RMC++ code had to be made; these are described in detail in the Supporting Information of ref 6. In short, an H-bonding cone was defined around each O−H group (as proposed in ref 2) as

$$r_{\mathrm{OO}} < r_{\mathrm{OO}}^{\max} - 0.00044\theta^2 \qquad (4)$$

where r_{OO} is the $O_1 \cdots O_2$ distance in angstroms considered to give an intact H-bond, θ is the $H-O_1 \cdots O_2$ angle (in degrees), where H is covalently bonded to O_1 and forms a (possible) H-bond with O_2, and $r_{\mathrm{OO}}^{\max}$ is a parameter that gives the range of the cone at a straight angle (i.e., for $\theta = 0$). Several cones with different values of $r_{\mathrm{OO}}^{\max}$ were used to steer the H-bonding

TABLE 2: H-Bond Statistics for the Different RMC Models According to the Geometric Criterion from Ref 2[a]

	HSMC	FREE	ASYM	MIX	SYM	SPCE	TIP4P-pol2
% ND	50	19	6	2	8	4	1
% SD	42	48	84	65	15	31	42
% DD	8	33	10	33	77	65	57
av	1.16	2.28	2.08	2.62	3.38	3.22	3.12

[a] The fluctuations in these numbers during the fits amount to a few percent. The last row shows the average number of H-bonds per molecule.

network to very different H-bond topologies. See the Supporting Information of ref 6 for details regarding the use of H-bonding geometrical constraints in RMC. The four different models are labeled FREE, with no imposed constraints on H-bonding; SYM, a maximally symmetric tetrahedral model; ASYM, with as large a fraction of the molecules as the data allow forced into asymmetric bonding situations; and MIX, where both asymmetric and four-coordinated constraints were used to create a mixture of the ASYM and the SYM models. Table 2 summarizes the H-bond populations of the different models calculated using $r_{OO}^{max} = 3.3$ Å; the different classes are nondonor (ND), single-donor (SD), and double-donor (DD) species. For comparison, the H-bond populations of the MD models investigated here are also presented in Table 2, together with results from a hard sphere Monte Carlo (HSMC) run. The HSMC model has been fit only to the internal geometry distributions and fixed minimum cutoffs between atoms, and thus provides a useful reference for the RMC models that also include diffraction data. Note that even though the SYM model according to the cone criterion has a larger amount of DD molecules compared to the MD models, it cannot be considered to be the more structured since the MD models have a larger fraction of even shorter and straighter H-bonds.

To control the internal distances in the water molecules, which is important since intramolecular scattering contributes significantly to the neutron diffraction patterns, distributions of internal O−H distances and H−O−H angles were implemented as additional data sets in the fitting. For all RMC runs, the internal distances and angles were set to fit Gaussian distributions approximating quantum distributions from path integral MD simulations by Stern and Berne,[10] using a full width at half-maximum (fwhm) of 0.15 Å for the distances and 21.6° for the angle distribution, centered at 0.98 Å and 105°, respectively.[10]

A fixed cutoff distance was used between atom pairs: 2.0, 0.79, and 1.0 Å for O−O, O−H, and H−H pairs, respectively (the low values of the O−H and H−H cutoff distances are needed to accommodate the intramolecular bonds). These cutoff radii are equivalent to a hard-sphere potential and were used in all the RMC fits; in EPSR the equivalent effect is obtained by introducing a strong repulsion at short internuclear distances.

C. MD Simulations. An SPC/E simulation with 2304 molecules and a box dimension of 41.041 Å was performed in the canonical ensemble at room temperature, 298 K. The TIP4P-pol2 structure is from Siepmann and co-workers and was generated at 300 K with 256 molecules.[8] Good statistics in the PPCFs could be obtained by averaging over a 1 ps trajectory with 1000 snapshots, but due to the limited size of the simulation, the PPCFs could only be obtained up to 9.863 Å. In order to calculate the total structure factors, the PSFs were first obtained by Fourier transformation of the PPCFs according to eq 1. The truncation error was investigated by truncating the SPC/E PCFs at different values of r_{max}, which showed that the limited r interval in the TIP4P-pol2 PCFs was not a source of error in the PSFs except at very low q. Both MD models reported here were rigid-molecule simulations. This means that the intramolecular contribution to the total structure factors is very distorted if one Fourier transforms the total O−H and H−H PPCFs, i.e., including the fixed intramolecular distances. Therefore, to treat the RMC and MD models on a completely even footing, the intramolecular part of the PPCFs from the RMC models was used also for the MD models. Since the intramolecular distributions in RMC are in agreement with distributions from path integral MD simulations, taking quantum effects into account this should provide the MD models with the optimal comparison with diffraction experiments.

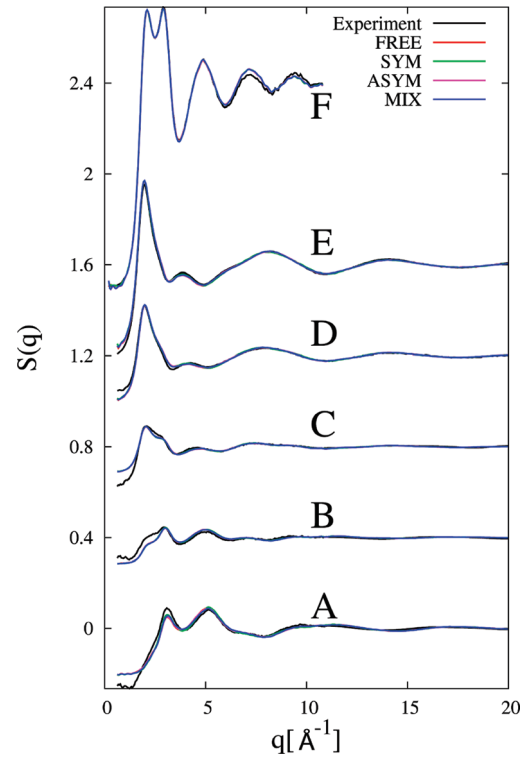

Figure 1. The fits of the different RMC models to ND data (A, 100% H_2O; B, 75% H_2O, 25% D_2O; C, 50% H_2O, 50% D_2O; D, 25% H_2O, 75% D_2O; E, 100 D_2O) and XD data (F, 100% H_2O). Note that the curves from all the RMC models coincide nearly perfectly.

Results and Discussion

A. Unconstrained RMC Model. The unconstrained RMC fit, labeled the FREE model, is a very direct and unbiased fit of a structure model to the neutron and X-ray diffraction data. Apart from the constraints imposed by the diffraction data, the only structural restrictions imposed are that the molecules should stay intact, that they not approach each other closer than the specified cutoff distances, and that their internal geometries should reproduce distributions acquired from path integral MD simulations. Thus, the results for the FREE model should reflect the real information content in the data and represent the most unconstrained fit satisfying elementary physical constraints. Figure 1 shows the results for the FREE model along with all the other RMC models. The fits for the different structure models are overall very good and strikingly similar with only very slight differences. For the ND data sets, it can be seen that the fit to the 100% D_2O data set is almost perfect. It is also seen that the fits get worse for the more hydrogen-rich isotopic mixtures. This is most easily explained by the significantly larger inelastic background correction for the more hydrogenous samples.

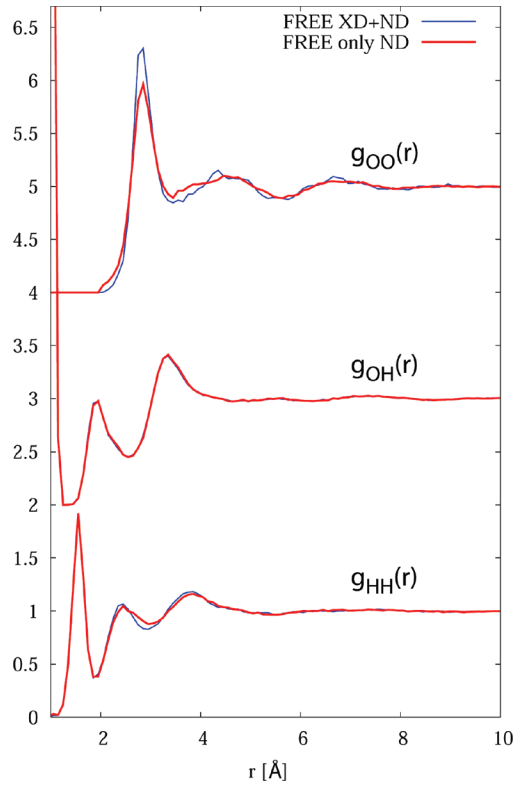

Figure 2. The $g(r)$ functions for the RMC-FREE model, with and without the X-ray diffraction (XD) data set.

Nonetheless, the fits to both the XD and ND data are quite good, and one can expect that a great deal of structural information can be successfully extracted.

In Figure 2 we show the PPCFs [O−O (top), O−H (middle), and H−H (bottom)] resulting from fitting the FREE model jointly to XD and ND data as well as a fit to only the ND data. We begin by discussing the joint XD and ND fits while the ND fits will be discussed below. Compared to structures from most MD water models, as well as previous experimentally derived PPCFs from either neutron diffraction[52] or X-ray diffraction,[7] the $g_{OO}(r)$ from the combined fit has a rather low first peak and shallower first minimum. Also, the second peak is well-defined with a sharp upper edge and a pronounced second minimum, and a small minimum is visible after the third shell; this is in agreement with the recent EPSR fit to the combined XD and ND data sets.[5] The $g_{OH}(r)$ and $g_{HH}(r)$ correlations shown beneath $g_{OO}(r)$ in Figure 2 also show some discrepancies with most MD models. Most notably, the O−H H-bonding peak, which in many MD models is observed at around $r = 1.75$ Å and with a height equal to or larger than that of the second O−H peak, is observed here to be both weaker in amplitude and shifted to almost 2 Å. Also the first intermolecular H−H peak is seen to be lower than determined before.[52] However, we have observed ambiguities in the data regarding the exact positions and amplitudes of the peaks in the PPCFs which will be highlighted in the next section. These results for the FREE model illustrate clearly, however, that well-defined and high peaks in the PPCFs are not particularly favored by the available diffraction data.

Turning now to the structural content of the ND data alone, we find that mainly the O−O PPCF is affected by the removal of the XD data from the RMC fit, as is clearly observed in Figure 2. The first peak in $g_{OO}(r)$ is reduced in height and becomes broader when the XD data is left out of the fit using RMC; in earlier fits to only the ND data using the EPSR approach, on the other hand, a significantly higher and sharper first O−O peak was reported for the same ND data set.[52] RMC and EPSR are, however, in agreement once both XD and ND data are used in the fit,[5,6] demonstrating that, in spite of the large O−O contribution to the scattering in the 25% D_2O sample, neutron diffraction alone is insufficient to determine the important O−O PPCF. All O−O PPCFs presented in this paper are thus to a large extent determined by the XD data. The O−H PPCF is, on the other hand, practically identical to the joint ND+XD fit, while the H−H PPCFs look very similar. It thus seems clear that including XD data is crucial for the determination of the O−O PPCF in spite of the large O−O contribution, in particular for the 50% and 25% D_2O data (cf. Table 1). The O−H and H−H PPCFs are however largely unaffected by the XD data, implying that all the information obtainable on these correlations are those shown in Figure 2. We note, finally, that removing the XD data from the fit makes the O−O PPCF smoother, while the O−H and H−H correlations are smooth also with the XD data included. For the O−O PPCF, the inclusion of the XD data brings, apart from a sharpening of the peaks, some oscillations and bumps. The bumpiness in the O−O PPCF is present in all the RMC models when the XD data are included, indicating that it derives somehow from the data. This may be caused by experimental errors or related to the finite q-interval giving an r-space resolution, which is insufficient to disallow narrow features in the O−O PPCF; the Fourier components of such features lie beyond the experimentally measured q-range. Significantly improved XD data are needed to determine these aspects of the O−O PPCF. In the next section, we will explore how well ND data actually determine the important H-bonding peak in $g_{OH}(r)$.

B. Differently H-Bonded RMC Models. The different structure models we have constructed should provide a test of the limits that diffraction data set for the structure of liquid water. The ASYM model was constructed to test how much asymmetry in the H-bonding configurations is actually allowed by the diffraction data and resembles the model suggested by Wernet et al.,[2] as well as the SD model of ref 6, but without the constraint to fit also the E-field from the TIP4P-pol2 structure. Similarly, the SYM model should reveal what constraints the data impose on the fraction of tetrahedrally H-bonded water molecules. This model is meant to correspond to the standard tetrahedral model of water, but again without the constraint to fit also the E-field from the TIP4P-pol2 structure. Finally, the MIX model has two completely different species, one highly asymmetric and the other very symmetric. This model resembles mixture models of water suggested earlier in the literature, for example, the flickering cluster model where a fraction of the molecules take part in strong hydrogen bonds while the others are less strongly H-bonded. Table 2 shows the fraction of H-bonds for the different structure models where the H-bond criterion of Wernet et al.[2] is used with $r_{OO}^{max} = 3.3$ Å (eq 4). Note that these numbers are not constant throughout the simulation runs but fluctuate by several percent around the values given. Despite the fluctuations, the four structure models have rather distinct H-bonding topologies. The SYM model is very symmetric, with around 80% of the molecules satisfying the DD criterion of ref 2. The ASYM model is about as asymmetric as the SYM model is symmetric. As reference values, Table 2 also shows the amount of H-bonds resulting from an RMC run with no diffraction data used, i.e., the HSMC model. This structure model is maximally disordered given the fixed cutoffs and the internal geometry distributions defining the water molecules. All H-bonds in the HSMC model are thus

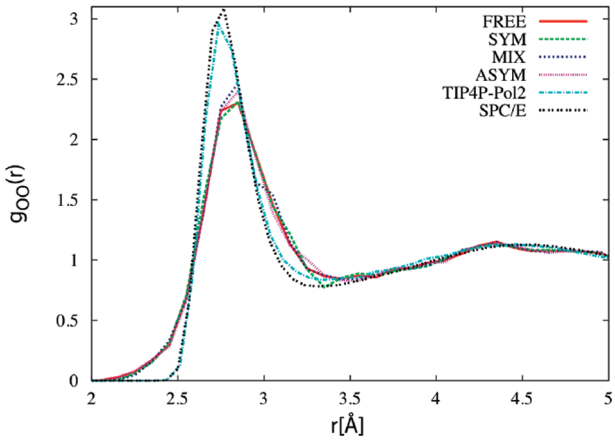

Figure 3. A zoomed-in view of the $g_{OO}(r)$ function for the RMC models and the SPC/E and TIP4P-pol2 model.

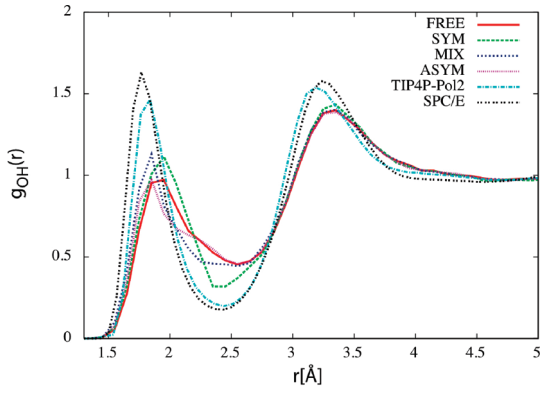

Figure 4. A zoomed-in view of the $g_{OH}(r)$ function for the RMC models and the SPC/E and TIP4P-pol2 model.

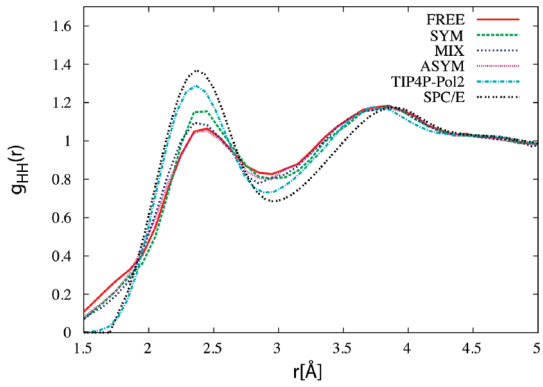

Figure 5. A zoomed-in view of the $g_{HH}(r)$ function for the RMC models and the SPC/E and TIP4P-pol2 model.

formed purely as a result of the density and nearest neighbor cutoff constraints. Consequently, the amount of H-bonding in the FREE model exceeding the corresponding number in the HSMC model cannot be random but reflects true information content of the data. The lack of orientational (many-body) correlations in the data, however, prevents firm determination of the number of H-bonds, as the following discussion will show.

In Figures 3−5, we report the PPCFs for the different RMC models as well as from MD simulations with the SPC/E and TIP4P-pol2 potential models, zoomed in on the important short-range correlations. As can be seen, the PPCFs look rather similar for all the RMC models, but important differences are nonetheless observed primarily in the O−H PPCF. Some bumpiness in the O−H PPCF for some of the models is due to the H-bond constraints; this is still beyond the resolution of the data in q-space, however. The first peak in $g_{OH}(r)$ is the one most directly influenced by the imposed H-bond constraints and thus understandably shows the largest variation. Its position ranges from around $r = 1.8$ Å for the MIX model to just below 2 Å for the SYM model, whereas its height is rather close to 1 for all models which, as should be noted, all reproduce the experiment in q-space. This is at odds with the MD models, which show shorter distances and higher peaks. The consequences of this for the agreement with the diffraction data will be discussed in the next section.

XD data are apparently completely insensitive to the number of H-bonds, since the O−O PPCFs look more or less identical for the different models, and as shown in the previous section, this is the only partial PCF that is significantly affected by XD data in RMC. The H−H PPCF is also very similar between the models, especially in terms of peak positions. The SYM model has a somewhat higher first peak, however. Again, the MD models show higher first intermolecular peaks at shorter distances for both the O−O and H−H PPCFs.

The respective fits in q-space in Figure 1 show the same goodness of fit, with only slight differences between different q-regions and data sets. This demonstrates that the diffraction data cannot distinguish between the observed differences in the PPCFs with any certainty, given that small experimental uncertainties are unavoidable, that the available q-range of the XD data is rather limited, and, furthermore, that above 8 Å^{-1} the ND data reflect mainly intramolecular structure, as will be stressed below; this is demonstrated by separately computing the scattering contribution from the individual molecules for which the internal O−H and H−H distance distributions follow the path integral MD simulation.[10] Despite the substantial structural differences between the models, only very minor variations are seen in q-space. It has been pointed out before in the literature,[6,37,42] and we obviously see again very clearly, that the PPCFs from diffraction data do not determine the orientational correlations in water sufficiently well to put any significant restrictions on the H-bonding statistics.

Finally, since all differently H-bonded structure models here reproduce the data equally well, one must say from a diffraction point of view, given the presently available data used in the fit, that all models here investigated are just as likely or unlikely to be representative of the real water structure. What one can say, however, is that in order to be consistent with the diffraction data used in these fits, the PPCFs should look similar to those shown in Figures 3−5. As will be shown below, this specifically applies to the position and height of the first O−O peak as well as the positions of the O−H and H−H peaks.

C. The MD Models. In Figures 3−5 we also depict the PPCFs of the two MD models under consideration. The comparison in r-space of the RMC and MD models shows that the first peak in $g_{OO}(r)$ for the RMC models is at slightly larger r than for the MD models. Furthermore, it is clearly much lower and broader than the corresponding MD peaks. This result agrees very well with a recent joint structure refinement of ND and XD data where the EPSR method was used, showing that MD models need softer potentials to reproduce experimental XD data.[5] Thus, it seems that different methods (RMC in the present work, as well as in ref 6 and EPSR[5]) together with different XD data sets (Narten and Levy[35] and Hura et al.[50]) converge to a picture where the first peak in $g_{OO}(r)$ has a height of around 2.3, significantly lower than for most MD models, in particular, the TIP4P-pol2 and SPC/E models that have a peak height of around 3.

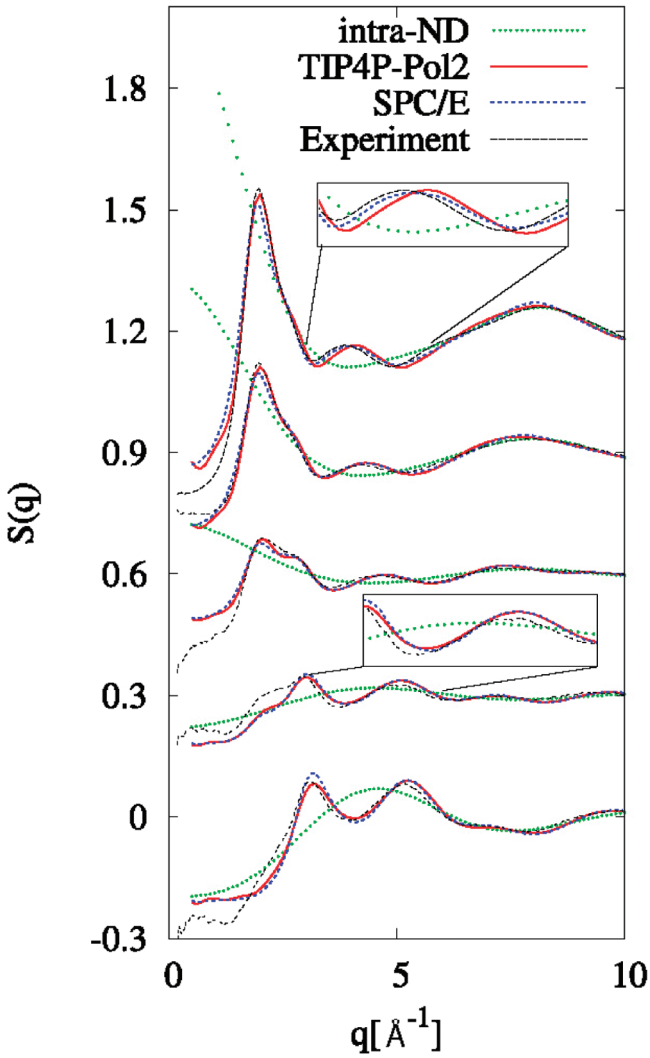

Figure 6. The comparison of SPC/E and TIP4P-pol2 to the ND data. The overlaid dots show the intramolecular contribution to the respective ND data sets. From the top: 100% D_2O; 75% D_2O, 25% D_2O; 50% D_2O, 50% D_2O; 25% D_2O, 75% D_2O; and 100% H_2O.

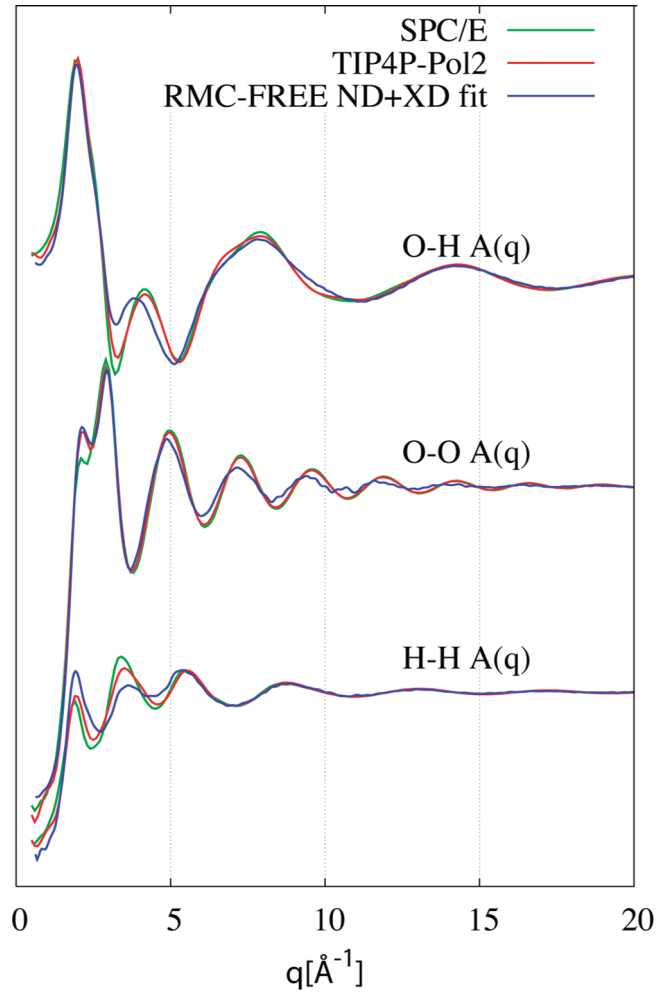

Figure 7. Comparison of the PSFs of water from the MD models and the RMC-FREE structure model.

As we stated in the Introduction, however, in order to avoid misinterpretations, the comparison should be done in q-space, where the data have been obtained. Figure 6 compares the calculated structure factors $S(q)$ for the SPC/E and the TIP4P-pol2 models with the neutron diffraction data sets. To aid in the analysis, we show on top of the ND data in Figure 6 the intramolecular contribution to these data sets from which it also becomes clear that beyond $q \sim 8$ Å^{-1} the scattering is mainly intramolecular; the intramolecular contribution was obtained from the internal O−H and H−H distributions in the model. Some evident discrepancies with experiment are observed when the MD models are taken to q-space. For reference, let us first recapitulate the conclusions drawn in ref 6 regarding the calculated X-ray $S(q)$ for these MD models and its comparison to experiment. Figures 6 and 7 of ref 6 showed that both MD models have a visible phase-shift to higher q above $q = 3.5$ Å^{-1} in comparison with XD data. This indicates directly that the mean distance to the first coordination shell in both models, manifested in the first peak in $g_{OO}(r)$, is too short; this is evident in Figure 3, where the PPCFs for the MD models are compared with their RMC counterparts. The too strong amplitude of the oscillation at higher q seen in the same figures (Figures 6 and 7 in ref 6) furthermore shows that the first peak is too high and narrow.

Moving on now to the comparison to the ND data, we see in Figure 6 that discrepancies in phase also show up in the ND data sets. The decomposed intramolecular contribution to the total neutron structure factors shown on top of the ND data sets can, together with the partial structure factors (PSFs) shown in Figure 7, be utilized to cast light on the observed deviations.[10] Note that Figure 6 illustrates an important fact regarding the ND data sets, namely, that many of its prominent features actually derive from the structurally less important intramolecular scattering; thus, not all peaks are equally important to reproduce by a structure model, given that a reliable representation of the intramolecular scattering contribution is used. First, since the oxygen−oxygen correlation dominates in the 25% D_2O data sets (as shown in Table 1), one can assign the apparent phase-shift above $q = 5$ Å^{-1} in the MD models to the O−O PSF, again indicating too short nearest-neighbor O−O distances, in agreement with the comparison to the XD data set discussed above. Figure 7 shows that the better fit of the RMC models to the 25% D_2O and XD data (as shown in Figures 6 and 7 of ref 6) is due to the O−O PSF; the MD models show a phase shift to higher q compared to the RMC-FREE model.

Second, TIP4P-pol2 is obviously worse off than SPC/E in describing the small second peak in the D_2O data set. This peak is actually the most important, since it reflects intermolecular structure, as Figure 6 reveals, whereas the region above $q = 5$ Å^{-1} is not interesting in this respect, since it is completely dominated by intramolecular scattering. Figure 7 shows that a

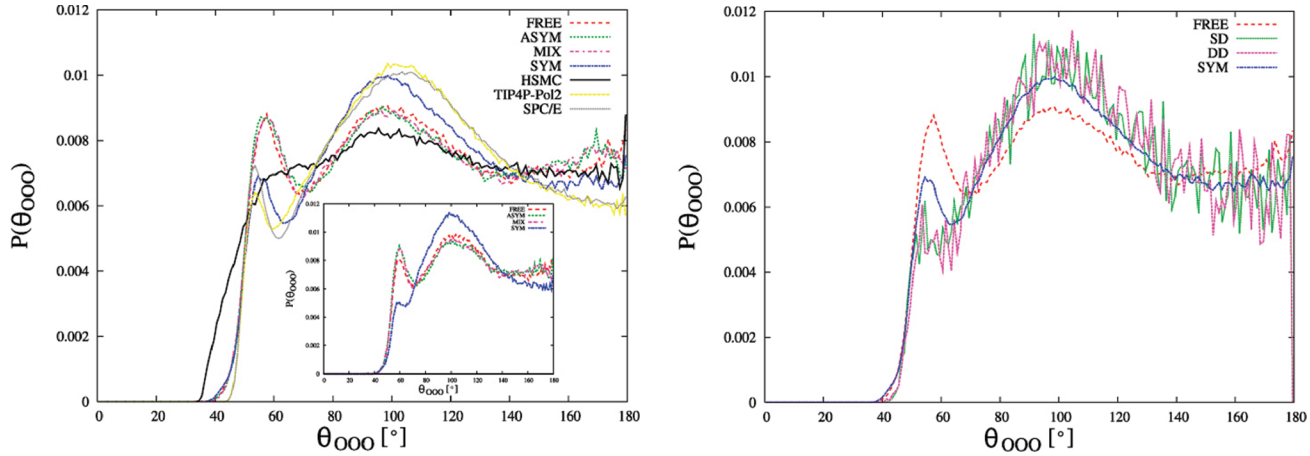

Figure 8. Distribution of $O_I-O_C-O_I$ angles. (a) The FREE, SYM, ASYM, and MIX structure models together with SPC/E and TIP4P-pol2, calculated with a radius of 3.4 Å. In the inset the distribution using the radius 3.18 Å as in ref 48 is shown. (b) The SD and DD structure models from ref 6.

phase shift in the H−H PSF lies behind the bad agreement for this peak; the O−H PSFs are very similar between SPC/E and TIP4P-pol2 and can therefore not be involved. This in turn can be traced back to inaccurate distances in the $g_{HH}(r)$ correlation; a comparison with the RMC models in Figure 5 shows that it must be the first intermolecular H−H peak. The 75% D_2O data shows a similar phase shift in the small second peak, albeit damped due to the lesser weight of the H−H partial in that data set. Finally, the peaks around $q = 3$ and 5 $Å^{-1}$ in the 100% H_2O data set correspond primarily to the O−H partial (added in negative, see Table 2), and the phase shifts of the MD models indicate too short intermolecular O−H distances, whereas the stronger amplitude for SPC/E corresponds to the higher O−H peaks in $g_{OH}(r)$.

For comparison, the RMC fits to the ND and XD data (Figure 1) suffer from none of the mismatches described above. The small second peak in the 100% D_2O data is well reproduced and no phase shifts are observed. In summary, since the RMC models all fit the diffraction data better than the MD models, especially with respect to the frequency of the oscillations in all data sets and the amplitude in $S_{XD}(q)$, one must conclude that the peak positions in the PPCFs for the RMC models are more consistent with experiment than those of the MD models, even though they still contain uncertainties.

D. O−O−O Angles. The distribution of $O_I-O_C-O_I$ angles provides a commonly used measure of three-body correlations and tetrahedrality in the oxygen (O_I) positions in the first coordination shell around the central water oxygen (O_C).[48,53,54] Assuming four nearest neighbors, a distribution peaking strongly around 109° would then indicate a tetrahedral distribution of oxygen positions, as is indeed very clearly the case for ice *Ih*. Note, however, that this does not imply a tetrahedral H-bonding situation, since no information about the H-bonding is included in this measure; in ref 6 we demonstrated that tetrahedrality in the H-bonding network was not given by the experimental data.[6] Here we will investigate to what extent experiment actually indicates the often assumed tetrahedrality of the oxygen sublattice.

We show in Figure 8a the distribution of first-coordination shell $O_I-O_C-O_I$ angles for each RMC structure and both MD models, calculated for all triplets within a radius of 3.4 Å around each oxygen atom and normalized to $\sin(\theta_{OOO})$, which is the distribution of randomly distributed $O_I-O_C-O_I$ angles. At this radius, which coincides with the first minimum in the O−O PPCF of the RMC structures, the coordination numbers of the PPCFs from both RMC and MD coincide with a value of ∼4.5. This radius was thus chosen in order to treat all structures on an equal footing.

The HSMC model, which is only constrained by the hard-sphere cutoffs and shown here as a reference point, shows a rather featureless distribution, which derives solely from the excluded volume around each molecule. It can be clearly seen that the other models fall into two classes. Qualitatively similar behavior is seen for the SYM model and both MD models, with a small sharp peak just below 60°, indicative of interstitial molecules from the second coordination shell, and a broad but strong maximum just below the tetrahedral angle of 109°. On the other hand, the distributions of $O_I-O_C-O_I$ angles for the FREE, ASYM, and MIX models are almost indistinguishable; all show a strong maximum around 60° and a weaker maximum around 100°. This clearly illustrates that the imposed H-bond constraints on the SYM model have made it very similar to the MD models with respect to the $O_I-O_C-O_I$ three-body angular correlation, whereas the other RMC models show significant deviations from tetrahedrality in the oxygen positions. Even though the SYM model has the same O−O PPCF as the other RMC structure models, its first coordination shell seems to have been strongly influenced by the imposed H-bond constraints. Hence we conclude that diffraction data on water is too insensitive to many-body correlations to put stronger restrictions on the tetrahedrality in the oxygen positions than what is observed in Figure 8a. Once again, the HSMC model provides a useful reference: the features seen for the FREE model arise solely from the fit to diffraction data, and only the imposition of constraints for 4-fold H-bond connectivity in the SYM model brings about a structure that is qualitatively similar to MD models. Note, however, that the SYM model differs from the MD models with respect to the distance correlations of the first coordination shell, as shown in Figures 3 and 4. In the inset of Figure 8a we show the distribution of angles for the RMC structures calculated instead with the radius 3.18 Å, as used in ref 48. At this shorter distance, the FREE model is seen to differ from the ASYM and MIX models, but the latter two still show very similar angle distributions, despite having different H-bond topologies.

In a recent study on the structural differences between heavy and light water,[48] the EPSR method was applied using XD and ND data on H_2O and D_2O separately with subsequent analysis in terms of $O_I-O_C-O_I$ angles. Interestingly, the SYM model in the inset of Figure 8a (where the same radius, 3.18 Å, has

TABLE 3: Values of the Tetrahedrality $\langle q \rangle$ Parameter in the Distributions of $O_1-O_C-O_1$ Angles, θ_{OOO}, for the Different Models (cf. Figure 8)[a]

model	SD	DD	FREE	SYM	ASYM	MIX	SPC/E	TIP4P-pol2	HSMC
$\langle q \rangle$	0.592	0.603	0.499	0.552	0.488	0.489	0.576	0.586	0.470

[a] A radius of 3.4 Å is used, as in Figure 8.

been used as in the EPSR study) has a closely similar angle distribution as that for D_2O derived in ref 48, even though the curve for H_2O is also rather similar. However, considering how significantly different the angle distributions are for the other RMC structure models, which equally well reproduce the experimental data, it seems difficult at present to attach much meaning to such fine details.

In Figure 8b we show the $O_1-O_C-O_1$ angle distribution of the two RMC models presented in ref 6 (labeled SD and DD), where also the *E*-field distribution from a TIP4P-pol2 MD simulation was included as an additional data set in the fit, and compare them with the FREE and SYM models. Despite the poor statistics, the inclusion of the MD-derived *E*-field can be seen to have had a major effect on the tetrahedrality in the oxygen positions of the SD and DD models. We reiterate that these models still differ substantially in their H-bond connectivity, the SD model having very asymmetric and nontetrahedral H-bonds, while the DD model has a strongly tetrahedral H-bond network. The effect of the TIP4P-pol2 *E*-field distribution on the oxygen three-body correlations is surprisingly large and may have introduced a bias in the fits, which, as mentioned before, may not be physical due to the inapplicability of this method for general structures.[11]

Although no unambiguous way exists to quantify tetrahedrality in a system from the distribution of O−O−O angles, a sometimes useful quantity is the $\langle q \rangle$ parameter[48,55] defined according to eq 5 to be 1 for a perfectly tetrahedral system.

$$\langle q \rangle = 1 - \left\langle \left(\cos(\theta_{OOO}) + \frac{1}{3} \right)^2 \right\rangle \qquad (5)$$

The $\langle q \rangle$ values for all discussed structures are presented in Table 3. The HSMC structure resulting from an RMC run with no fitted diffraction data gives a $\langle q \rangle$ value of 0.470. It is important here to realize the arbitrariness of the scale. While $\langle q \rangle = 1$ for a perfectly tetrahedral system, the value to which the structuring effect from diffraction data should be referenced is thus 0.470. The SPC/E and TIP4P-pol2 MD models give 0.576 and 0.587 respectively; these models are considered to give tetrahedral structures, both in terms of H-bonds and O−O−O angles. Hence, values around 0.6 can be considered to represent a fair amount of tetrahedrality in the oxygen positions.

With the relative scale thus determined, we consider the RMC structure models. As expected from Figure 8, the $\langle q \rangle$ values of the FREE, ASYM, and MIX models are very similar but still surprisingly close to the HSMC value. The structure models (SD and DD) from ref 6 are, on the other hand, even slightly more tetrahedral in the O−O−O correlation than the MD models, and the SYM structure model presented here is comparable. It is thus clear that diffraction data do not impose strong constraints on tetrahedrality in the oxygen positions; it is only when H-bond tetrahedrality is imposed by geometrical constraints (SYM) or an *E*-field distribution from an MD simulation is enforced (SD and DD), or else when an underlying potential (MD, EPSR) is assumed, that structural solutions with a high degree of O−O−O tetrahedrality arise.

The emergence of a broad peak centered at 100° for the FREE, ASYM, and MIX models can be reduced to an interpretation in terms of distorted locally tetrahedral O−O−O order, but the width of the peak allows a vast range of different local structures, including various extreme structures that cannot be considered tetrahedral.

Conclusions

In the present work we have analyzed what bounds, in terms of PPCFs, O−O−O angles, and H-bond coordination, the X-ray and neutron diffraction data, separately and in combination, actually set on structure models of water. We find that the H-bond connectivity is not given by the data except as very broad bounds; the average number of H-bonds per molecule calculated with the cone criterion of ref 2 ranging from 2.08 to 3.38. The four different models (FREE, SYM, ASYM, and MIX) all describe the diffraction data in *q*-space to an equal goodness of fit and lead to very similar O−O PPCFs, which, however, have significantly lower and broader peaks than obtained from the SPC/E and TIP4P-pol2 MD force-fields; the position of the first peak is furthermore at slightly longer distance than obtained from MD simulations. The O−H PPCF shows a greater variation between the models due to the flexibility allowed by the data in this correlation, which underlines that new data are required to put further constraints on the important O−H peaks.

Considering the similarity of the O−O PPCFs, it may be surprising that the distributions of O−O−O angles can differ to the observed extent. There seems to be minimum structural information from the data on the O−O−O angles, as seen in the comparison to the HSMC structure. Only with the imposition of tetrahedral H-bond constraints or an MD-derived *E*-field distribution in RMC was the O−O−O tetrahedrality seen to qualitatively reproduce that of the MD models.

As an illustration of the importance of making all comparisons with diffraction data in *q* space, which corresponds to the real experimental data, we performed detailed comparisons of the SPC/E and TIP4P-pol2 models directly with the experimental data. From this we concluded that the peak positions and amplitudes in *r*-space need to be more similar to our RMC-determined counterparts for an improved representation of the data. Phase shifts and amplitude discrepancies in *q*-space indicate that the MD peak positions in *r*-space are at too short distance and the heights are too large.

The broad range in H-bond connectivity allowed by the present data sets arises from the inherent insensitivity to many-body correlations of the diffraction data, as required to define H-bond connections. Additional information might be gained from extending the X-ray diffraction data to higher *q*, but for the neutron data, the intramolecular scattering dominates already for $q \sim 8$ Å^{-1}, which limits the structure information at higher *q*. It is clear that, in order to experimentally put stronger bounds on structure models of water, complementary experimental techniques need to be applied. In this context, recent applications of synchrotron radiation spectroscopies, such as X-ray absorption (XAS),[2,29,56] emission (XES),[1,17,57] and photoemission,[58−62] provide new unique information, although a consensus still needs to be reached as to the exact interpretation of these new experimental data.

Acknowledgment. We are grateful to A. K. Soper for supplying the neutron data, to T. Head-Gordon for making the X-ray diffraction data available and to J. I. Siepmann for sending the TIP4P-pol2 MD trajectory. This work was supported by the Swedish Foundation for Strategic Research, the Swedish Research Council (VR), and the National Science Foundation (US) CHE-0518637 and CHE-0431425. A generous grant of CPU time from the Swedish NSC center is gratefully acknowledged. Portions of this research were carried out at the Stanford Synchrotron Radiation Laboratory, a national user facility operated by Stanford University on behalf of the U.S. Department of Energy, Office of Basic Energy Sciences.

References and Notes

(1) Tokushima, T.; Harada, Y.; Takahashi, O.; Senba, Y.; Ohashi, H.; Pettersson, L. G. M.; Nilsson, A.; Shin, S. *Chem. Phys. Lett.* **2008**, *460*, 387.
(2) Wernet, P.; Nordlund, D.; Bergmann, U.; Cavalleri, M.; Odelius, M.; Ogasawara, H.; Näslund, L. Å.; Hirsch, T. K.; Ojamäe, L.; Glatzel, P.; Pettersson, L. G. M.; Nilsson, A. *Science* **2004**, *304*, 995.
(3) Sorenson, J. M.; Hura, G.; Glaeser, R. M.; Head-Gordon, T. *J. Chem. Phys.* **2000**, *113*, 9149.
(4) Head-Gordon, T.; Hura, G. *Chem. Rev.* **2002**, *102*, 2651.
(5) Soper, A. K. *J. Phys.: Condens. Matter* **2007**, *19*, 335206.
(6) Leetmaa, M.; Wikfeldt, K. T.; Ljungberg, M. P.; Odelius, M.; Swenson, J.; Nilsson, A.; Pettersson, L. G. M. *J. Chem. Phys.* **2008**, *129*, 084502.
(7) Hura, G.; Russo, D.; Glaeser, R. M.; Head-Gordon, T.; Krack, M.; Parrinello, M. *Phys. Chem. Chem. Phys.* **2003**, *5*, 1981.
(8) Chen, B.; Xing, J. H.; Siepmann, J. I. *J. Phys. Chem. B* **2000**, *104*, 2391.
(9) Fecko, C. J.; Eaves, J. D.; Loparo, J. J.; Tokmakoff, A.; Geissler, P. L. *Science* **2003**, *301*, 1698.
(10) Stern, H. A.; Berne, B. J. *J. Chem. Phys.* **2001**, *115*, 7622.
(11) Ljungberg, M. P.; Nilsson, A.; Pettersson, L. G. M. Unpublished, 2008.
(12) Röntgen, W. C. *Ann. Phys.* **1892**, *45*, 91.
(13) Morgan, J.; Warren, B. E. *J. Chem. Phys.* **1938**, *6*, 666.
(14) Bernal, J. D.; Fowler, R. H. *J. Chem. Phys.* **1933**, *1*, 515.
(15) Cavalleri, M.; Odelius, M.; Nordlund, D.; Nilsson, A.; Pettersson, L. G. M. *Phys. Chem. Chem. Phys.* **2005**, *7*, 2854.
(16) Eaves, J. D.; Loparo, J. J.; Fecko, C. J.; Roberts, S. T.; Tokmakoff, A.; Geissler, P. L. *Proc. Natl. Acad. Sci. U.S.A.* **2005**, *102*, 13019.
(17) Fuchs, O.; Zharnikov, M.; Weinhardt, L.; Blum, M.; Weigand, M.; Zubavichus, Y.; Bär, M.; Maier, F.; Denlinger, J. D.; Heske, C.; Grunze, M.; Umbach, E. *Phys. Rev. Lett.* **2008**, *100*, 027801.
(18) Head-Gordon, T.; Johnson, M. E. *Proc. Natl. Acad. Sci. U.S.A.* **2006**, *103*, 7973.
(19) Head-Gordon, T.; Johnson, M. E. *Proc. Natl. Acad. Sci. U.S.A.* **2007**, *103*, 16614.
(20) Head-Gordon, T.; Rick, S. W. *Phys. Chem. Chem. Phys.* **2007**, *9*, 83.
(21) Hetényi, B.; De Angelis, F.; Giannozzi, P.; Car, R. *J. Chem. Phys.* **2004**, *120*, 8632.
(22) Leetmaa, M.; Ljungberg, M.; Ogasawara, H.; Odelius, M.; Näslund, L. Å.; Nilsson, A.; Pettersson, L. G. M. *J. Chem. Phys.* **2006**, *125*, 244510.
(23) Nilsson, A.; Wernet, P.; Nordlund, D.; Bergmann, U.; Cavalleri, M.; Odelius, M.; Ogasawara, H.; Näslund, L.-Å.; Hirsch, T. K.; Ojamäe, L.; Glatzel, P.; Pettersson, L. G. M. *Science* **2005**, *308*, 793.
(24) Näslund, L. Å.; Lüning, J.; Ufuktepe, Y.; Ogasawara, H.; Wernet, P.; Bergmann, U.; Pettersson, L. G. M.; Nilsson, A. *J. Phys. Chem. B* **2005**, *109*, 13835.
(25) Odelius, M.; Cavalleri, M.; Nilsson, A.; Pettersson, L. G. M. *Phys. Rev. B* **2006**, *73*, 024205.
(26) Paesani, F.; Iuchi, S.; Voth, G. A. *J. Chem. Phys.* **2007**, *127*, 074506.
(27) Pettersson, L. G. M.; Tokushima, T.; Harada, Y.; Takahashi, O.; Shin, S.; Nilsson, A. *Phys. Rev. Lett.* **2008**, *100*, 249801.
(28) Prendergast, D.; Galli, G. *Phys. Rev. Lett.* **2006**, *96*, 215502.
(29) Smith, J. D.; Cappa, C. D.; Messer, B. M.; Drisdell, W. S.; Cohen, R. C.; Saykally, R. J. *J. Phys. Chem. B* **2006**, *110*, 20038.
(30) Smith, J. D.; Cappa, C. D.; Wilson, K. R.; Cohen, R. C.; Geissler, P. L.; Saykally, R. J. *Proc. Natl. Acad. Sci. U.S.A.* **2005**, *102*, 14171.
(31) Smith, J. D.; Cappa, C. D.; Wilson, K. R.; Messer, B. M.; Cohen, R. C.; Saykally, R. J. *Science* **2004**, *306*, 851.
(32) Soper, A. K. *J. Phys.: Condens. Matter* **2005**, *17*, S3273.
(33) Tokmakoff, A. *Science* **2007**, *317*, 54.
(34) Winter, B.; Aziz, E. F.; Hergenhahn, U.; Faubel, M.; Hertel, I. V. *J. Chem. Phys.* **2007**, *126*, 124504.
(35) Narten, A. H.; Levy, H. A. *Science* **1969**, *165*, 447.
(36) McGreevy, R. L.; Pusztai, L. *Mol. Simul.* **1988**, *1*, 359.
(37) Jedlovszky, P.; Bakó, I.; Pálinkás, G.; Radnai, T.; Soper, A. K. *J. Chem. Phys.* **1996**, *105*, 245.
(38) Jedlovszky, P.; Brodholt, J. P.; Bruni, F.; Ricci, M. A.; Soper, A. K.; Vallauri, R. *J. Chem. Phys.* **1998**, *108*, 8528.
(39) Pusztai, L. *Phys. Rev. B* **1999**, *60*, 11851.
(40) Soper, A. K. *Chem. Phys.* **1996**, *202*, 295.
(41) Berendsen, H. J. C.; Grigera, J. R.; Straatsma, T. P. *J. Phys. Chem.* **1987**, *91*, 6269.
(42) McGreevy, R. L. *J. Phys.: Condens. Matter* **2001**, *13*, R877.
(43) McLain, S. E.; Imberti, S.; Soper, A. K.; Botti, A.; Bruni, F.; Ricci, M. A. *Phys. Rev. B* **2006**, *74*, 094201.
(44) Toth, G.; Baranyai, A. *J. Chem. Phys.* **1997**, *107*, 7402.
(45) Toth, G.; Baranyai, A. *Mol. Phys.* **1999**, *97*, 339.
(46) Hart, R. T.; Benmore, C. J.; Neuefeind, J. C.; Kohara, S.; Tomberli, B.; Egelstaff, P. A. *Phys. Rev. Lett.* **2005**, *94*, 047801.
(47) Hart, R. T.; Mei, Q.; Benmore, C. J.; Neuefeind, J. C.; Turner, J. F. C.; Dolgos, M.; Tomberli, B.; Egelstaff, P. A. *J. Chem. Phys.* **2006**, *124*, 134505.
(48) Soper, A. K.; Benmore, C. J. *Phys. Rev. Lett.* **2008**, *101*, 065502.
(49) Nilsson, A.; Ogasawara, H.; Cavalleri, M.; Nordlund, D.; Nyberg, M.; Wernet, P.; Pettersson, L. G. M. *J. Chem. Phys.* **2005**, *122*, 154505.
(50) Hura, G.; Sorenson, J. M.; Glaeser, R. M.; Head-Gordon, T. *J. Chem. Phys.* **2000**, *113*, 9140.
(51) Evrard, G.; Pusztai, L. *J. Phys.: Condens. Matter* **2005**, *17*, S1.
(52) Soper, A. K. *Chem. Phys.* **2000**, *258*, 121.
(53) Chau, P.-L.; Hardwick, A. J. *Mol. Phys.* **1998**, *93*, 511.
(54) Errington, J. R.; Debenedetti, P. G. *Nature (London)* **2001**, *409*, 318.
(55) Chau, P.-L.; Hardwick, A. J. *Mol. Phys.* **1998**, *93*, 511.
(56) Myneni, S.; Luo, Y.; Näslund, L. Å.; Cavalleri, M.; Ojamäe, L.; Ogasawara, H.; Pelmenschikov, A.; Wernet, P.; Väterlein, P.; Heske, C.; Hussain, Z.; Pettersson, L. G. M.; Nilsson, A. *J. Phys.: Condens. Matter* **2002**, *14*, 213.
(57) Guo, J. H.; Luo, Y.; Augustsson, A.; Rubensson, J. E.; Såthe, C.; Ågren, H.; Siegbahn, H.; Nordgren, J. *Phys. Rev. Lett.* **2002**, *89*, 137402.
(58) Winter, B.; Weber, R.; Widdra, W.; Dittmar, M.; Faubel, M.; Hertel, I. V. *J. Phys. Chem. A* **2004**, *108*, 2625.
(59) Winter, B.; Hergenhahn, U.; Faubel, M.; Björneholm, O.; Hertel, I. V. *J. Chem. Phys.* **2007**, *127*, 094501.
(60) Nordlund, D.; Ogasawara, H.; Bluhm, H.; Takahashi, O.; Odelius, M.; Nagasono, M.; Pettersson, L. G. M.; Nilsson, A. *Phys. Rev. Lett.* **2007**, *99*, 217406.
(61) Winter, B.; Aziz, E. F.; Hergenhahn, U.; Faubel, M.; Hertel, I. V. *J. Chem. Phys.* **2007**, *126*, 124504.
(62) Nordlund, D.; Odelius, M.; Bluhm, H.; Ogasawara, H.; Pettersson, L. G. M.; Nilsson, A. *Chem. Phys. Lett.* **2008**, *460*, 86.

JP9007619